Research Article | Vol. 28, No. 4 / 17 February 2020 / Optics Express 5706
Optics EXPRESS

4-channel 200 Gb/s WDM O-band silicon photonic transceiver sub-assembly

MILTIADIS MORALIS-PEGIOS,[1,*] STELIOS PITRIS,[1] THEONI ALEXOUDI,[1] NIKOS TERZENIDIS,[1] HANNES RAMON,[2] JORIS LAMBRECHT,[2] JOHAN BAUWELINCK,[2] XIN YIN,[2] YOOJIN BAN,[3] PETER DE HEYN,[3] JORIS VAN CAMPENHOUT,[3] TOBIAS LAMPRECHT,[4] ANDREAS LEHNMAN,[5] AND NIKOS PLEROS[1]

[1]*Department of Informatics, Aristotle University of Thessaloniki, Thessaloniki, Greece*
[2]*Ghent University IMEC, IDLab, Department of Information Technology, B-9052 Ghent, Belgium*
[3]*IMEC, Kapeldreef 75, Leuven B-3001, Belgium*
[4]*Vario-optics ag, 9410 Heiden, Switzerland*
[5]*Amphenol FCI, Berlin, Germany*
[*]*mmoralis@csd.auth.gr*

Abstract: We demonstrate a 200G capable WDM O-band optical transceiver comprising a 4-element array of Silicon Photonics ring modulators (RM) and Ge photodiodes (PD) co-packaged with a SiGe BiCMOS integrated driver and a SiGe transimpedance amplifier (TIA) chip. A 4×50 Gb/s data modulation experiment revealed an average extinction ratio (ER) of 3.17 dB, with the transmitter exhibiting a total energy efficiency of 2 pJ/bit. Data reception has been experimentally validated at 50 Gb/s per lane, achieving an interpolated 10E-12 bit error rate (BER) for an input optical modulation amplitude (OMA) of −9.5 dBm and a power efficiency of 2.2 pJ/bit, yielding a total power efficiency of 4.2 pJ/bit for the transceiver, including heater tuning requirements. This electro-optic subassembly provides the highest aggregate data-rate among O-band RM-based silicon photonic transceiver implementations, highlighting its potential for next generation WDM Ethernet transceivers.

1. Introduction

The new era of disaggregated data centers (DC) [1] in conjunction with the ceaseless growth of intra DC traffic [2], calls for advances in the deployed optical transceiver technologies that have now to offer increased operational speed and aggregate bandwidth in a low power and footprint envelope. Demarcating, however, from the currently deployed 100 (4×25) Gb/s Ethernet (GbE) modules towards 200 GbE and even 400 GbE interfaces, necessitates multi-channel transceiver configurations with line rates equal to or even higher than 50 Gb/s, exploiting either wavelength division (WDM) or space division multiplexing (SDM). Silicon photonics (SiPho) stand out as a technology enabler, with previous demonstrations in the C-band [3–5] having already achieved 8×40G [3] operation in optical transmitter (Tx) layouts, while complete C-band transceiver modules incorporating both the Tx and receiver (Rx) circuits together with their electronic driver and TIA blocks have reached 4-lane WDM setups with a rather moderate aggregate bandwidth of 80 Gb/s [5].

With O-band having, however, turned into the dominant spectral region in the high-speed intra-DC interconnect segment, research efforts have gradually shifted towards O-band TxRx implementations [6–9]. So far, the main focus has been primarily on the Tx part when equal or higher than 25 Gb/s line rate operation is targeted [10–15], with both single and multi- channel Tx layouts reporting up to 400 Gb/s aggregate bandwidths when exploiting either travelling wave Mach Zehnder modulator (MZM) arrays [9,10] or Si-based RMs [11–15]. The recently

#373454 https://doi.org/10.1364/OE.373454
Journal © 2020 Received 30 Jul 2019; revised 1 Dec 2019; accepted 11 Dec 2019; published 14 Feb 2020

Optics EXPRESS

demonstrated MZM-based transmitters comprised, however, just the silicon photonic chip using externally connected and bulky electrical drivers, requiring a rather higher driving voltage of 2.9V and additional digital signal processing [9] that bring its energy consumption rather away from the low-power specifications of intra-DC transmitter requirements. MZM-based transmitter co-assembled with their electronic drivers were also demonstrated, reaching only 2-lane layouts with a total of 2×56 Gb/s aggregate capacity [10]. RM-based Tx layouts offer significant footprint and energy advantages compared to MZMs, with our recent work on the first WDM Si-Pho O-band Tx reporting a 4×40Gb/s setup with just 2.2 pJ/bit energy consumption [14], lacking, however, a co-integrated Rx part to turn it into a complete WDM TxRx sub-assembly.

In this paper, we extend our previous work on RM-based WDM optical Txs [14] and demonstrate a complete 200 Gb/s capable O-band WDM transceiver sub-assembly that performs at 50 Gb/s linerates and offers the highest aggregate bandwidth among the so far reported Si-Pho RM-based O-band transceiver layouts. It comprises a SiPho 4-channel transceiver chip co-packaged with its electronics onto a polymer-based circuit board, with its 4-channel electronic driver and TIA circuits having been fabricated in a 55 nm SiGe technology platform. The SiPho Tx part comprises 4 high-speed carrier depletion RMs followed by a 4-channel ring-based multiplexer (MUX), while the Rx part incorporates a similar 4-channel de-multiplexer (DEMUX) followed by 4 Ge photodiodes. A 4×50 Gb/s data modulation experiment is presented using four different wavelengths at 2 nm channel spacing, revealing open eye-diagrams with extinction ratio (ER) values between 3 dB and 3.38 dB. The electronic drivers deliver an average of 2 Vpp to each RM and consume only 244 mW, translating to an energy efficiency of 1.22 pJ/bit, that increases to 2 pJ/bit when taking into account the RM thermal tuning mechanism. Moreover, 2×50 Gb/s data reception operation is presented, revealing error free operation with an interpolated bit error ratio of 10 E-12, referenced to an input OMA of −9.5 dBm. The TIAs consume 448 mW, corresponding to a power consumption of 2.24 pJ/bit and concluding to a total transceiver efficiency of 4.24 pJ/bit at 50Gb/s.

2. Device fabrication and description

A schematic of the 4-channel WDM O-band transceiver is depicted in Fig. 1(a) along with a microscope photo of the device mounted on a polymer board and a close up of the Silicon and electronics part illustrated in Figs. 1(b) and 1(c), respectively. The transceiver assembly comprises a SiPho chip (14,04 mm^2), wire-bonded to a SiGe electronic driver array (2,4 mm^2) and a SiGe transimpedance amplifier array (2,9 mm^2), with all three chips mounted on a polymer based printed circuit board (PCB).

The SiPho chip was fabricated in imec's ISIPP50G platform and incorporates a 4-channel transmitter (Tx) array, based on Micro-Ring-Modulators (MRMs) and a 4-channel receiver (Rx) array, based on SiGe photodiodes [11]. Each Tx cell comprises a 7.5 μm carrier-depletion RM, featuring 45 fF capacitance, a Q factor of ~5000, a 3-dB bandwidth of 33.8 GHz and an FSR of 9.0 nm. An integrated heater allows fine tuning of the RM resonance and is accessible through electrical DC pads at the east side of the chip. The optical outputs from all four RMs are multiplexed in a 4-channel MUX unit, based on cascaded double-ring resonators, comprising two micro-rings for each MUX channel [16], featuring an FSR of 9.0 nm, while a collective heater allows thermal tuning of the MUX's transfer function. Optical input/output access to the integrated Tx array is achieved via TE-polarization grating couplers (GC) at the west side of the chip, based on PDK-ready imec designs and designated in Fig. 1(b) as Tx In 1-4 and Tx out, referring to the 4 Tx inputs and the combined Tx output, respectively. Each Rx cell comprises a Ge waveguide photodetector (PD), featuring a 3db bandwidth of 50 GHz, a capacitance of 30 fF and a responsivity of 0.9 A/W. The Rx array is designed to facilitate a common WDM optical input, comprising 4 signals in different wavelengths, with a channel spacing of 2 nm, that is demultiplexed in a 4-channel DEMUX unit, based on cascaded double-ring resonators similar to

Optics EXPRESS

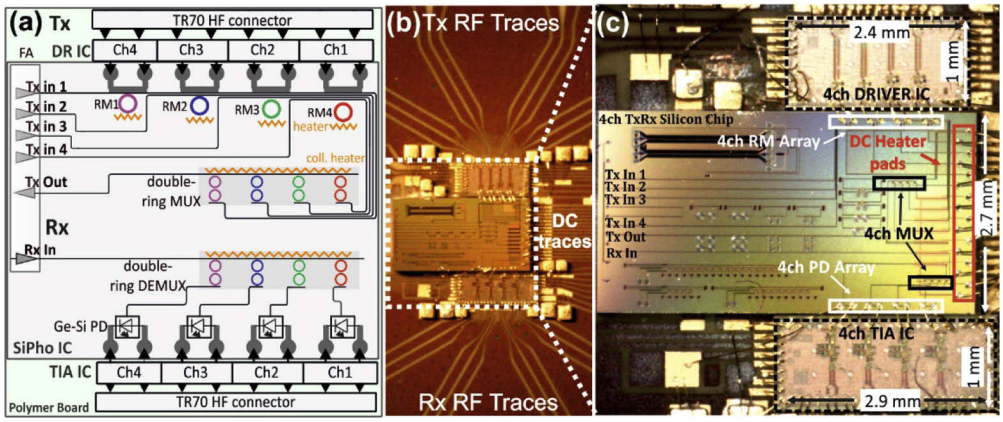

Fig. 1. (a) Schematic diagram of the 200 Gb/s transceiver (b) Macroscopic view of the assembled transceiver illustrating the SiPho photonic chip, the SiGe driver and TIA electronic circuitry mounted on a polymer board (c) Close-up view of the Si and electronic chips.

the one employed on the Tx. The demultiplexed signals are waveguided to the individual Rx cells, while access to the Rx array is achieved through a TE-polarization GC, at the west side of the chip, denoted as RxIn in Fig. 1(b).

The transceiver's electronic circuity comprises a 4-channel fully differential electronic driver array [17] and a 4-channel fully differential TIA array [18], both fabricated in a 55 nm SiGe BiCMOS technology. The 4-channel electronic driver provides 2 Vpp to each RM, while combined power consumption for all channels was measured at 244 mW, that effectively translates to a power efficiency value of 1.22 pJ/bit at 50 Gb/s. Moreover, it employs a lumped driving scheme, by leveraging the short electrical connections (wirebonds) between the driver and RM pads, thus avoiding the use of termination resistors resulting in increased energy efficiency. An unbalanced output stage is also exploited, to allow DC-coupling to the modulator without an external bias-tee, significantly reducing real-estate and cost of the resulting Tx. The 4-channel TIA features differential sensing of the photocurrent, significantly improving the sensitivity of the Rx, while the use of an on-chip bias network also provides bias voltage to the PD minimizing the assembly procedure. The TIA circuitry consumes, all channels combined, 448 mW, resulting in an efficiency of 2.24 pJ/bit at 50 Gb/s.

All three chips were mounted on a high frequency printed circuit board, facilitating the necessary electronic components required for the operation of the driver and TIA circuitry (e.g. decoupling capacitors, wire-bonding pads, power supply I/O pins) and the routing of the driver's input and TIA's output signals, through 50GHz electrical traces. It should be noted, that the employed circuit boards were specifically developed as part of an iterative approach of developing an electro-optical circuit board (EOCB), that would eventually allow both electrical routing and optical waveguiding and coupling, through low-loss optical polymer waveguides and silicon to polymer adiabatic couplers, respectively. Moreover, the copper traces provide nearly vertical sidewalls and well controlled gap width, yielding low impedance variations and allowing features size down to 40μm. The high-speed routing credentials of the polymer RF traces, have already been validated in previous demonstrations, achieving seamless electrical transmission of 112 Gb/s PAM-4 signals through 4cm long lines [19]. Finally, the electronic and photonic chips were placed in close proximity, in order to minimize the wire bonding induced inductance, while a specially designed layout allowed seamless connectivity to the driver inputs and TIA outputs through the use of solderless RF connectors (Ardent TR70).

Optics EXPRESS

3. Experimental setup and results

A schematic of the 200 Gb/s Tx part of the transceiver in conjunction with the experimental setup employed for assessing its performance is illustrated in Fig. 2. A bit pattern generator was used to generate a differential signal of an NRZ pseudo-random binary sequence (PRBS7-1) at 50 Gb/s, with a peak amplitude of 180 mV, that was applied to the driver's inputs through TR70 pluggable RF connectors. The electronic driver circuitry was powered by four voltage supplies. i.e. VddPre, Vdd, Vbias1 and Vbias2, with the first associated with the pre-driver operation, the second corresponding to the main supply voltage and the last two employed for setting the bias point of the RMs. The operational settings of the integrated drivers were fine tuned for each RM, in order to provide the best performance in terms of modulation depth and optical eye diagram opening. A tunable laser source (TLS) was used to sequentially generate one of the 4 CW signals, at $\lambda 1 = 1309.70$ nm, $\lambda 2 = 1311.90$ nm, $\lambda 3 = 1314.26$ nm and $\lambda 4 = 1316.34$ nm, according to the RM operating points. The CW signals were injected through a fiber array at the input GCs, corresponding to Tx In1-4, respectively. A polarization controller was used to match the incoming light's polarization to the grating couplers. The resulting modulated signal was coupled out of the chip through an output grating coupler (Tx out) and after amplification in a semiconductor optical amplifier (SOA), it was injected in an optical bandpass filter (OBPF) with 0.5 nm 3 dB-bandwidth, to filter out the SOA amplified spontaneous emission (ASE). Finally, the signal was evaluated in a sampling oscilloscope (OSC).

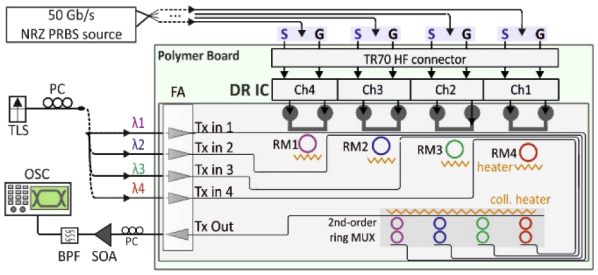

Fig. 2. Schematic and experimental setup used for Tx characterization.

Figure 3(a)-(e) illustrates the spectral transfer function of the 4-channel MUX obtained by sequentially sweeping each Tx input port with a TLS and measuring the optical power at the common Tx Out port. The MUX featured a free spectral range (FSR) of 9.02 ± 0.2 nm, and a channel spacing of 2 ± 0.2 nm, while the insertion loss was 10-12 dB, deviating from the expected specifications of 1-2 dB, due to a design error. The wavelength annotations ($\lambda 1$-$\lambda 4$) in Fig. 3(a) indicate the MUX channels that were used for data transmission, while Figs. 3(b)–3(e) depict the output spectra of the respective MUX channels before and after tuning the respective RM resonances inside the MUX transfer function. The 4ch-DEMUX at the Rx side followed the exact same design, as the one employed at the Tx side, and follows the same spectral characteristics in terms of channel spacing and FSR.

The performance of the 4-channel Tx was assessed via a 4×50 Gb/s NRZ OOK data modulation experiment. Figures 3(f)–3(i) illustrate the optical eye diagrams, obtained at the common output port of the MUX, with each RM sequentially tuned at the appropriate wavelength, revealing ER values of 3.07 dB, 3.25 dB, 3.38 dB and 3.01 dB, respectively. The RMs were driven with approximately 2 Vpp, provided by the integrated driver array with each driver input fed by a 180-mVpp differential signal, and the RMs DC reverse biased at −0.39 V, −0.41 V, −0.42 V, −0.38 V, respectively. The optical power of the CW signal injected at all four wavelengths of the transmitter ($\lambda 1$-$\lambda 4$), was 10 dBm, while the average optical power of the resulting modulated signals emerging at the common output port, were −17.7 dBm, −18 dBm, −19.1 dBm and −19

Optics EXPRESS

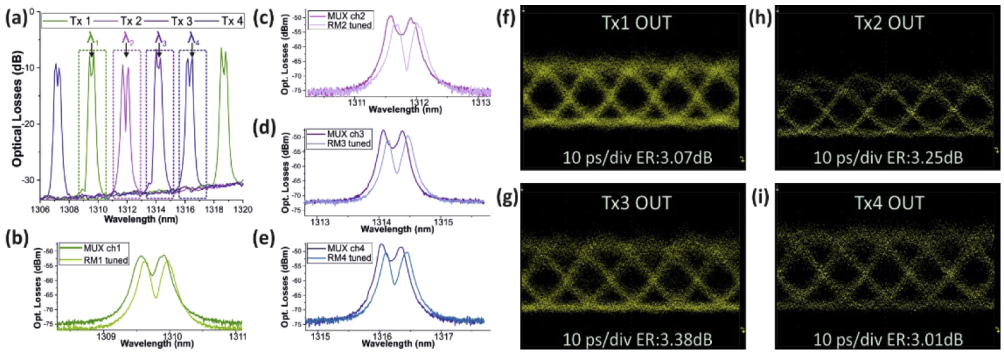

Fig. 3. (a) Optical Spectra of the 4-channel MUX (b)-(e) Tx out channel#1-4 spectra before and after tuning RM#1-4 resonance to the nearest respective MUX channel#1-4 (f),(g),(h),(i) Eye diagrams of the Tx 4×50 Gb/s operation.

dBm, respectively. Breaking down the optical losses, the two GCs imposed ~9 dB, the RM insertion losses ranged between 6-9 dB, depending on the Tx channel and operating wavelength, while the MUX introduced ~10-12 dB of optical losses, being mainly the result of a MUX design error. The SOA was electrically driven at 276 mA, providing an average gain of 20 ± 2dB, depending on the operating wavelength. In order to tune the RM resonances, to the respective MUX channel, the electrical powers applied to the integrated heater of RM1-RM4 were 39.3 mW, 47.58 mW, 33.63 mW and 38.75 mW, respectively. The power consumption of the driver array was 244 mW, corresponding to a high energy efficiency of 1.22 pJ/bit, and concluding to a total Tx power efficiency of 2 pJ/bit when factoring in the RM heater consumption. It should be noted, that the on-chip temperature and consequentially the RM operating points were kept stable through the use of a Thermo Electric Controller (TEC) that consumed ~180 mW. Next iterations of the transceiver could be benefit from lower power consumption associated with RM monitor and control by exploiting the recently introduced ContactLess Integrated Photonic Probe (CLIPP) system [20], to allow stabilization of the RM operation, while increasing the power consumption by only ~0.5 pJ/bit at 50 Gb/s data rates.

Figure 4(a) illustrates the experimental setup employed for the characterization of the Rx part of the transceiver. The TIA circuitry was powered through two voltage supplies, with one (Vdd1 = 1V) utilized for providing power to an on-chip programmable register that allows fine tuning of the TIA properties, and the other (Vdd = 2.5V) utilized for powering up the TIAs and for biasing of the PDs. A bit pattern generator was used to generate a differential signal of an NRZ pseudo-random binary sequence (PRBS7-1) at 40 Gb/s and 50 Gb/s, with a peak amplitude of 300 mV, that was amplified by a commercial high-speed RF driver amplifier to drive a 30 GHz O-band MZM modulator. In order to determine the peak spectral points of the 4-ch DEMUX, light from a TLS, was swept across the O-band and subsequently injected to the MZM modulator, with the resulting modulated signal coupled to the common RxIn port. An RF-power meter was used to monitor the electrical outputs of the TIAs and as such determine the peak transmission points of each MUX channel. Based on these measurements the peak wavelengths of Rx channels 2 and 3 were 1316.6 nm and 1318.79 nm. Unfortunately, channels 1 and 4 had their wire-bonds to their TIAs cut and could not be evaluated, while the design error in the MUX/DEMUX design prevented the usage of the collective DEMUX heater to match the transmitter and receiver channel wavelengths, as its use significantly increased the DEMUX insertion loss. A TLS was used to subsequently generate the two CW signals at 1316.6 nm and 1318.79 nm that correspond to Rx2 and Rx3 channels, respectively, and were injected to the MZM modulator. The resulting modulated optical signal was amplified in a SOA for compensating the MZM, MUX and GC

Optics EXPRESS

optical loss and was coupled through the respective GC to the common input port of the Rx array, i.e. RxIn, after being filtered in an OBPF with 0.5 nm 3 dB-bandwidth. Finally, the electrical TIA output signals were routed through high speed RF traces to TR70 pluggable connectors and were subsequently monitored and evaluated in a real time OSC.

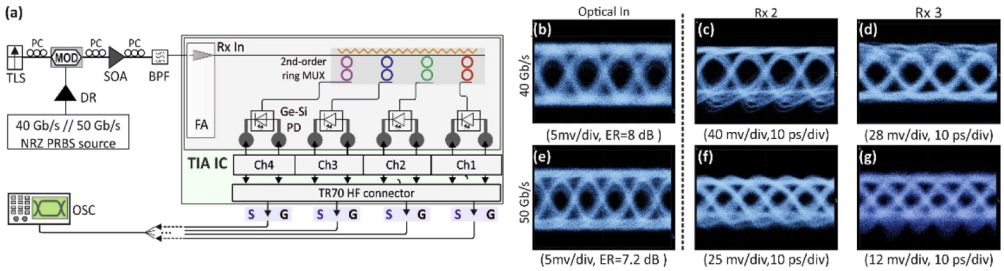

Fig. 4. (a) Schematic and experimental setup used for Tx characterization (b)-(e) Input Optical eye diagram at 40 Gb/s – 50 Gb/s (c)-(f), (d)-(g) Ch2, Ch3 single-ended TIA output at 40 Gb/s-50 Gb/s.

The performance of the two Rx channels was assessed with 40 Gb/s and 50 Gb/s NRZ OOK data. Figures 4(b) and 4(e) illustrate the optical eyes at the MZM modulator output at λ=1316.6 nm, featuring an ER of 8 dB and 7.2 dB at 40 Gb/s and 50 Gb/s, respectively, with their OMA being 5.4 dBm and 6 dBm, respectively, at the BPF output and prior being injected at the Rx common input (RxIn). Taking into account the ~4.5 dB losses induced by the GC and the ~11 dB extra losses from the DEMUX, the optical signal at the PD 's input finally had an OMA of −10.1 dBm and −9.5 dBm, at 40 Gb/s and 50 Gb/s, respectively. The single-ended TIA outputs were connected to a real time OSC, that provided an indication of the signal quality through BER estimation. The electrical eye diagrams depicted in Figs. 4(c), (f)-(d), (g) correspond to a BER of 10E-12, at 40 Gb/s and 50 Gb/for Rx channels 2 and 3, respectively. The 10E-12 BER value was interpolated by measuring zero errors over a sequence of 3E + 07 bits via the toolkit provided by the Real-Time Oscilloscope, subsequently applying the interpolation methodology described in [21]. More specifically, a 0.86dB optical attenuation was introduced before the signal reaches the RTO, which can be mapped to an SNR degradation from 13.8 dB to 11.2 dB, and a theoretical BER of 1E-12 to 1E-7, respectively, based on the assumption that thermal Gaussian noise at the input of the receiver is the dominant cause of errors in the system. After inserting the attenuation factor the 3.01E-07 bits measurement was repeated, revealing again zero errors and allowing interpolation to a BER of 1E-12. Finally, in case the optical signal originated from the transceiver's Tx side and as such had an ER of 3 dB at 50 Gb/s, the average power of the optical signal being injected in the receiver should be increased by 3.2 dB, as compared to the experimentally demonstrated case featuring a 7.2 dB ER, in order to achieve the same OMA and performance. The TIA array power consumption was measured to be 448 mW, resulting to a power efficiency of 2.44 pJ/bit at 50 Gb/s.

In order to assess the transceiver's maximum achievable transmission distance, the total optical power budget was calculated and is illustrated in Table 1. As can be easily observed, the main source of optical loss originates from the MUX and respective DEMUX, and can be easily corrected in subsequent fabrication runs to reach the initially targeted 1-2 dB losses that have been experimentally verified in respective C-band designs [16]. This indicates that a loss-optimized future run employing GC based on previous C-band designs with 2 dB losses [22] and optimized RM structures with 4 dB losses [23] can allow for total optical losses of 10 dB for the Tx side and 4 dB for the receiver side. Considering an input laser power of 10 dBm and talking into account the 3 dB ER achieved by the RM, the OMA of the modulated signal at the Tx egress would be −1.76 dBm. As such, the OMA of the signal at the receiver PD-TIA would be −5.76

Optics EXPRESS

dBm, featuring a ~4 dB power margin as compared to the receiver −9.5 dBm OMA requirement at 50 Gb/s. Finally, taking into account the very low dispersion of single mode standard fiber (SSMF) in the O-band spectral window, and the typical optical losses of about 0.33 dB/km [24], the optical power margin of 4 dB allows transmission over 11.5 km of SSMF, including the 0.2 dB optical connector associated losses.

Table 1. Breakdown of optical power budget.

	Transmitter			Receiver	
	GCs	RM	MUX	GC	DEMUX
Current Run	9 dB	6 dB	10-12 dB	4.5 dB	10-12 dB
Optimized Run	4 dB	4 dB	2 dB	2 dB	2 dB

To evaluate the TxRx performance when multi-channel operation is targeted, we developed a simulation framework, that takes into account both the electrical crosstalk originating from the RF routing of the electrical signals and the optical crosstalk originating from the finite crosstalk of the employed MUX and DEMUX. Based on the electrical simulation results, performed in Keysight's ADS, both the differential-mode-to-mode and the common-mode-to-differential mode crosstalk was −40 dB and as such don't affect the electrical performance of the 4-channel TxRx. Considering the optical crosstalk originating from finite crosstalk of the optical MUX and DEMUX the optical performance of the multichannel TxRx operation, was simulated using the VPI software suite. The measured optical transfer functions of the MUX and DEMUX, along with the Tx and Rx performance, were imported into a custom simulation environment, with the worst-case optical crosstalk measured to be 22 dB and the Tx ER set to 3 dB at 50 Gb/s. BER measurements at 50 Gb/s performed by gradually injecting a modulated signal to each MUX channel and as such emulating the TxRx with one up to all four-channel operating simultaneously revealed a power penalty of 0.2 dB at 10E-12 ratio for simultaneous 4-channel versus single channel operation.

To conclude, Table 2 summarizes the measured performance and compares with previous CMOS-SiPho TxRx demonstrations revealing the low-power high bandwidth credentials of this work.

Table 2. O-band transceivers performance comparison.

	This work	[7]	[8]	[9]
Year	2019	2015	2013	2019
Photonic Electronic Integration Scheme	Wire-bonding	Monolithic	Wafer-to-wafer	N/A
Line Rate	50 Gb/s	25 Gb/s	5 Gb/s	100 Gb/s
Aggregate BW	200 Gb/s	100 Gb/s	5 Gb/s	400 Gb/s
Multiplexing	DWDM	CWDM	N/A	SDM
Transmitter				
Type	RM	MZM	RM	MZM
ER	3.17 dB	4.5 dB	>10 dB	N/A
Consumption	2 pJ/bit	5.4 pJ/bit	0.89 pJ/bit	N/A
Receiver				
Sensitivity at line rate	−9.5 dBm	N/A	−8 dBm	1.5 dBm
Consumption	2.2 pJ/bit	N/A	0.44 pJ/bit	N/A

Optics EXPRESS

4. Conclusion

We demonstrated a 200 Gb/s O-band 4-chanel silicon photonic WDM optical transceiver, comprising a SiPho chip co-assembled with a 4-ch electronic driver and a 4-ch TIA onto a single polymer-based board. The high speed and low power credentials of the integrated TxRx are validated through 50 Gb/s per lane modulation and data reception experiments, yielding a total transceiver energy efficiency of 4.4 pJ/bit.

Funding

H2020 LEIT Information and Communication Technologies (ICT- MASSTART (825109), ICT-STREAMS(688172)); Staatssekretariat für Bildung, Forschung und Innovation (15.0339-1).

Disclosures

The authors declare no conflicts of interest.

References

1. N. Terzenidis, M. Moralis-Pegios, G. Mourgias-Alexandris, T. Alexoudi, K. Vyrsokinos, and N. Pleros, "High-Port and Low-Latency Optical Switches for Disaggregated Data Centers: The Hipoλaos Switch Architecture," IEEE J. Opt. Commun. Netw. **10**(7), B102–B116 (2018).
2. Cisco, "Cisco Global Cloud Index: Forecast and Methodology, 2015–2020," White Pap. (2015).
3. R. Ding, Y. Liu, Q. Li, Z. Xuan, Y. Ma, Y. Yang, A. Eu-Jin Lim, G.-Q. Lo, K. Bergman, T. Baehr-Jones, and M. Hochberg, "A Compact Low-Power 320-Gb/s WDM Transmitter Based on Silicon Microrings," IEEE Photonics J. **6**(3), 1–8 (2014).
4. J. Du, L. Zheng, K. Xu, G. Chen, L. Ma, Y. Liu, and Z. He, "High speed and small footprint silicon micro-ring modulator assembly for space-division-multiplexed 100-Gbps optical interconnection," Opt. Express **26**(11), 13721–13729 (2018).
5. M. Rakowski, M. Pantouvaki, P. De Heyn, P. Verheyen, M. Ingels, H. Chen, J. de Coster, G. Lepage, B. Snyder, K. De Meyer, M. Steyaert, N. Pavarelli, J. Su Lee, P. O'Brien, P. Absil, and J. Van Campenhout, "A 4×20Gb/s WDM ring-based hybrid CMOS silicon photonics transceiver," *2015 IEEE International Solid-State Circuits Conf. (ISSCC)*, 1–3 (2015).
6. T. Alexoudi, N. Terzenidis, S. Pitris, M. Moralis-Pegios, P. Maniotis, C. Vagionas, C. Mitsolidou, G. Mourgias-Alexandris, G. T. Kanellos, A. Miliou, K. Vyrsokinos, and N. Pleros, "Optics in Computing: From Photonic Network-on-Chip to Chip-to-Chip Interconnects and Disintegrated Architectures," J. Lightwave Technol. **37**(2), 363–379 (2019).
7. J. C. Rosenberg, F. Horst, M. Khater, F. G. Anderson, R. Leidy, T. Barwicz, D. Gill, E. Kiewra, Y. Martin, J. S. Orcutt, A. D. Stricker, C. Whiting, K. McLean, B. Porth, C. Xiong, N. Feilchenfeld, K. Giewont, K. Nummy, B. J. Offrein, W. Haensch, and W. M. J. Green, "Monolithic Silicon Photonic WDM Transceivers," *European Conf. on Opt. Commun. (ECOC)*, Gothenburg, 1–3 (2017).
8. C. Li, R. Bai, A. Shafik, E. Z. Tabasy, G. Tang, C. Ma, C.-H. Chen, Z. Peng, M. Fiorentino, P. Chiang, and S. Palermo, "A ring-resonator-based silicon photonics transceiver with bias-based wavelength stabilization and adaptive-power-sensitivity receiver," *IEEE International Solid-State Circuits Conf.*, 124–125 (2013).
9. E. El-Fiky, A. Samani, Md S. Alam, M. Sowailem, O. Carpentier, M. Jacques, L. Guenin, D. Patel, and D. Plant, "A 4-Lane 400 Gb/s Silicon Photonic Transceiver for Intra-Datacenter Optical Interconnects," *2019 Opt. Fiber Commun. Conf. and Exhibition (OFC)*, 1–3 (2019).
10. G. Denoyer, C. Cole, A. Santipo, R. Russo, C. Robinson, L. Li, Y. Zhou, J. Chen, B. Park, F. Boeuf, S. Crémer, and N. Vulliet, "Hybrid Silicon Photonic Circuits and Transceiver for 50 Gb/s NRZ Transmission Over Single-Mode Fiber," J. Lightwave Technol. **33**(6), 1247–1254 (2015).
11. J. Van Campenhout, Y. Ban, P. De Heyn, A. Srinivasan, J. De Coster, S. Laredenois, B. Snyder, S. Balakrishnan, G. Lepage, N. Golshani, S. Jannsen, A. Lesniewska, K. Croes, A. Miller, P. Verheyen, M. Pantouvaki, and P. Absil, "Silicon Photonics for 56G NRZ Optical Interconnects," *Opt. Fiber Commun. Conf.*, W1I.1 (2018).
12. H. Li, G. Balamurugan, M. Sakib, J. Sun, J. Driscoll, R. Kumar, H. Jayatilleka, H. Rong, J. Jaussi, and B. Casper., "A 112 Gb/s PAM4 Transmitter with Silicon Photonics Microring Modulator and CMOS Driver," *Opt. Fiber Commun. Conf.* Postdeadline Papers, Th4A.4 (2019).
13. M. Moralis-Pegios, S. Pitris, T. Alexoudi, H. Ramon, X. Yin, J. Bauwelinck, Y. Ban, P. De Heyn, J. Van Campenhout, and N. Pleros, "52 km-Long Transmission Link Using a 50 Gb/s O-Band Silicon Microring Modulator Co-Packaged With a 1V-CMOS Driver," IEEE Photonics J. **11**(4), 1–7 (2019).
14. M. Moralis-Pegios, S. Pitris, T. Alexoudi, N. Terzenidis, H. Ramon, J. Lambrecht, J. Bauwelinck, X. Yin, Y. Ban, P. De Heyn, J. Van Campenhout, T. Lamprecht, A. Lehnman, and N. Pleros, "A 160 Gb/s (4×40) WDM O-band Tx

Optics EXPRESS

subassembly using a 4-ch array of Silicon Rings co-packaged with a SiGe BiCMOS IC driver," accepted at *European Conf. on Opt. Commun.*, (2019).
15. M. Wade, M. Davenport, M. De Cea Falco, P. Bhargava, J. Fini, D. Van Orden, R. Meade, E. Yeung, R. Ram, M. Popović, V. Stojanović, and C. Sun, "A Bandwidth-Dense, Low Power Electronic-Photonic Platform and Architecture for Multi-Tbps Optical I/O," *European Conference on Optical Communication (ECOC)*, 1–3 (2018).
16. P. De Heyn, J. De Coster, P. Verheyen, G. Lepage, M. Pantouvaki, P. Absil, W. Bogaerts, J. Van Campenhout, and D. Van Thourhout, "Fabrication-Tolerant Four-Channel Wavelength-Division-Multiplexing Filter Based on Collectively Tuned Si Microrings"," J. Lightwave Technol. **31**(16), 2785–2792 (2013).
17. H. Ramon, J. Lambrecht, J. Verbist, M. Vanhoecke, S. A. Srinivasan, P. De Heyn, J. Van Campenhout, P. Ossieur, X. Yin, and J. Bauwelinck, "70 Gb/s Low-Power DC-Coupled NRZ Differential Electro-Absorption Modulator Driver in 55 nm SiGe BiCMOS," J. Lightwave Technol. **37**(5), 1504–1514 (2019).
18. J. Lambrecht, H. Ramon, B. Moeneclaey, P. Ossieur, P. De Heyn, J. Van Campenhout, J. Bauwelinck, and X. Yin, "90-Gb/s NRZ Optical Receiver in Silicon Using a Fully Differential Transimpedance Amplifier," J. Lightwave Technol. **37**(9), 1964–1973 (2019).
19. T. Lamprecht, F. Betschon, J. Lambrecht, H. Ramon, X. Yin, A. Bruderer, and R. Premerlani, "EOCB-Platform for Integrated Photonic Chips Direct-on-Board Assembly within Tb/s Applications," *2018 IEEE 68th Electronic Compon. and Technol. Conf. (ECTC)*, 854–858 (2018).
20. P. Ciccarella, M. Carminati, G. Ferrari, D. Bianchi, S. Grillanda, F. Morichetti, A. Melloni, and M. Sampietro, "Impedance-Sensing CMOS Chip for Noninvasive Light Detection in Integrated Photonics," IEEE Trans. Circuits Syst. II: Express Briefs **63**(10), 929–933 (2016).
21. HFTA-010.0: Physical Layer Performance: Testing the Bit Error Ratio (BER) available online : https://pdfserv.maximintegrated.com/en/an/3419.pdf
22. D. Vermeulen, S. Selvaraja, P. Verheyen, G. Lepage, W. Bogaerts, P. Absil, D. Van Thourhout, and G. Roelkens, "High-efficiency fiber-to-chip grating couplers realized using an advanced CMOS-compatible Silicon-On-Insulator platform," Opt. Express **18**(17), 18278–18283 (2010).
23. J. Van Campenhout, Y. Ban, P. De Heyn, A. Srinivasan, J. De Coster, B. Snyder, S. Balakrishnan, G. Lepage, N. Golshani, S. Janssen, K. Croes, A. Miller, P. Verheyen, M. Pantouvaki, and P. Absil, "Silicon Photonics for 56G NRZ Optical Interconnects," *Opt. Fiber Commun. Conf.* W1I.1 (2018).
24. Corning SMF-28e Optical Fiber Product Information (2007), retrieved http://www.princetel.com/datasheets/smf28e.pdf